Dynamic micromechanical measurement of the flexural modulus of micrometre-sized diameter single natural fibres using a vibrating microcantilever technique

Ali Reda, Thomas Dargent, Steve Arscott

Dynamic micromechanical measurement of the flexural modulus of micrometre-sized diameter single natural fibres using a vibrating microcantilever technique

Ali Reda, Thomas Dargent and Steve Arscott

University of Lille, CNRS, Centrale Lille, University Polytechnique Hauts-de-France, UMR 8520-IEMN, F-59000 Lille, France.

E-mail: steve.arscott@univ-lille.fr

Abstract

The dynamic response of a structure is a manifestation of its inherent characteristics, including material density, mechanical modulus, thermo- and viscoelastic properties, and geometric properties. Together, these factors influence how the material behaves in dynamic scenarios, dictating its damping properties and behaviour under varying forces. In this study we present a novel approach to accurately determine the flexural (bending) modulus of microscopic diameter natural fibres (flax) using microcantilever vibration analysis. Traditionally, the characterisation of the mechanical properties of fibres has relied on macroscopic methods such as tensile testing, which often results in high scatter in measurement data; furthermore, tensile testing does not accurately represent microscale or dynamic conditions and can be complex in terms of sample preparation and loading. To address this, we have developed a microscale technique involving the fabrication of microcantilevers using flat polypropylene support chips, inspired by microelectromechanical systems (MEMS) approaches. Our method provides a refined method for accurately characterising the mechanical modulus of flax fibres, with reduced data dispersion compared to traditional macroscopic testing. Furthermore, by reducing the influence of inherent fibre defects and maintaining homogeneity along the length of the fibre, our micro-scale technique provides reliable modulus determination. This work opens avenues for improved understanding and application of natural and man-made fibres, such as glass and optical fibres, in a variety of fields.

1.Introduction

In the field of materials science, the determination of mechanical properties has historically relied on macroscopic vibrational methods to provide insight into various material behaviours. Such methods have been used extensively to investigate the dynamic mechanical properties of composite materials

in industrial applications [1], structural membranes [2], and even natural materials such as bone [3]. In addition, vibration methods have been widely used to evaluate the sound absorption and vibration damping properties of fibre composites, including glass fibres and natural flax fibres [4]. Moreover, numerical models based on natural frequency measurements from these techniques have been instrumental in assessing physical and mechanical properties, such as Young's modulus, in various materials [5]. On a smaller scale, microelectromechanical systems (MEMS) and nanoelectromechanical systems (NEMS) have emerged as powerful tools for characterising mechanical properties at the micro- and nanoscale. These methods have been applied to the study of single crystal silicon, silicon-based materials [6] and diamond [7]. Recent studies using micro-cantilevers have further explored the application of vibration methods to the quantification of the behaviour of representative MEMS devices [8,9]. For example, microcantilevers have been used to analyse the mechanical properties of single crystal silicon (SSC) using vibration methods [10]. In addition, vibrational methods have found utility in macroscopic cantilevers, allowing the detection of local stiffness variations in materials and structures [11]. The vibrational modes of atomic force microscope cantilevers have been used to study sample surfaces, adding to the versatility of these methods in materials characterisation [12]. Despite the wide applicability of vibration methods, the accurate determination of mechanical properties in fibres, particularly at the microscale, remains a challenge. Macroscale tensile testing has been a common approach to determining fibre properties, but often results in relatively highly scattered experimental results [13–17]. In particular, there has been a lack of microscale methods capable of accurately assessing the flexural modulus of fibres. Specifically, high speed camera equipment to characterise a vibrating cantilever has been used to determine the mechanical properties of materials on macroscopic [18], microscopic [10], and nanoscopic scales [19] for applications ranging from sport [20] to plant mechanics [21,22]. In terms of characterizing plants using cantilever techniques, Schramm *et al.* [23] measured the elastic modulus of a vibrating wheat straw. Shioya *et al.* [24] measured the mechanical properties of long stems of *Cyperus malaccensis* using high speed camera observation. To our knowledge, there has been no work concerning the transient response (using vibrational studies of cantilevers) of a single fibre-based microcantilever using high speed photography to capture the deflection.

In this article, we present a novel approach that overcomes the limitations of macroscopic testing by introducing a microcantilever-based vibration method for single fibres. We demonstrate how this method allows the precise determination of the flexural (bending) modulus of microscopic diameter natural fibres (flax). By taking advantage of the microcantilever technology, we demonstrate the effectiveness of this technique in accurately quantifying the mechanical properties of fibres at the microscale. Our findings contribute to the advancement of microscale material

characterisation techniques and pave the way for a deeper understanding of the mechanical behaviour of natural fibres, with potential implications for various applications in industries such as composites, textiles and biomedical materials.

2.Modelling

The resonant frequency f (first mode) of a cantilever is given by [25,26]:

$$f = \frac{\alpha_1^2}{2\pi}\sqrt{\frac{E_f I}{mL^4}} \tag{1}$$

Where α_1 is a constant equal to 1.875104, E_f is the flexural modulus, I is the second moment of area in the direction of the cantilever length, m is the mass per unit length of the cantilever, and L is the cantilever length.

For a cantilever having a hollow circular cross section with an outer diameter d_o and an inner diameter d_i, the second moment of area I is given by:

$$I = \frac{\pi}{64}(d_o^4 - d_i^4) \tag{2}$$

The mass per unit length m is given by:

$$m = \frac{\pi}{4}(d_o^2 - d_i^2)\rho \tag{3}$$

Substituting, simplifying, and rearranging allows us to write the bending modulus E_f of a hollow fibre cantilever as:

$$E_f = \left(\frac{2\pi f}{\alpha_1^2}\right)^2 \frac{16\rho L^4}{d_o^2 + d_i^2} \tag{4}$$

And for a solid fibre cantilever, we have:

$$E_f = \left(\frac{2\pi f}{\alpha_1^2}\right)^2 \frac{16\rho L^4}{d_o^2} \tag{5}$$

Therefore, in principle, if we carefully measure the cantilever's dimensions, its density, and its resonant frequency, we can in principle experimentally determine its flexural modulus.

3.Experimental

In order to experimentally test the idea of a fibre-based cantilever we chose flax fibres as the test vehicle. Retted flax samples (Family: *Linaceae*, Genus: *Linum* Species: *L. usitatissimum*, Variety:

Felice) were collected from a field belonging to the company Van Robaeys Frères (Killem, France). To conduct this research, individual single flax fibres were carefully removed from the external tissue of the flax plant stem using a methodical manual peeling technique developed by the authors–ensuring minimal mechanically-induced defect formation. This involved making a small break at the top of the stem to separate the outer tissue from the inner part. With the aid of a pair of precision tweezers, straight bundles of fibres were carefully peeled from the outer tissue whilst avoiding bending of the fibres. The extraction of individual flax fibres was then carried out under a microscope with a large working distance to facilitate manipulation. Once a single straight flax fibre was identified within the bundle, it was carefully peeled using precision tweezers. The single fibres were then cut and placed on a polished silicon wafer–this gave a large visual contrast between the microscopic single fibres and the silicon surface. A method was then employed by the authors to carefully position individual single flax fibres onto flat polypropylene support chips. Figure 1 shows the fabrication method of the cantilever/polypropylene chip samples.

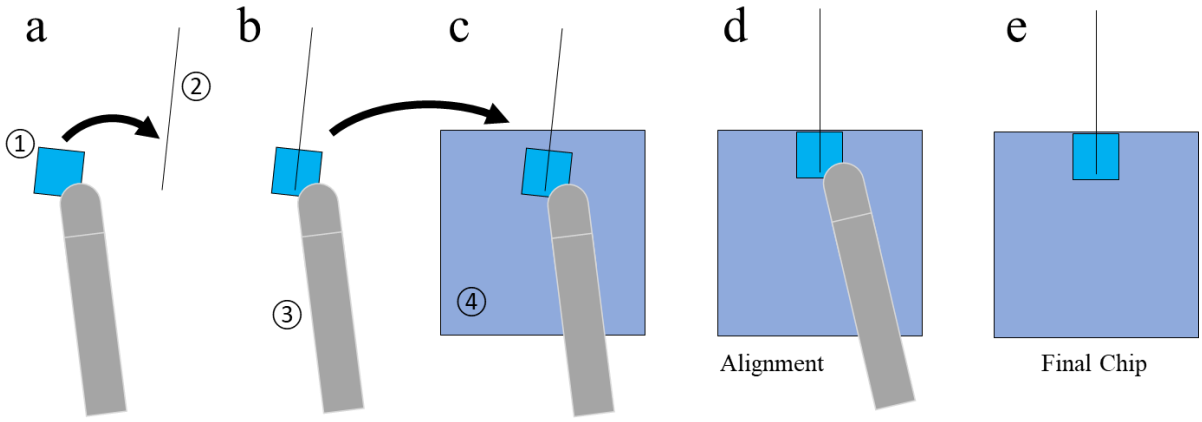

Figure 1. Schematic diagram of the main fabrication steps to produce the single fibre-based cantilevers plus support chips. ① adhesive tape (2 mm by 2 mm), ② single flax fibre, ③ tweezers, ④ polypropylene support chip (6 mm × 6 mm × 100 µm).

First, the single fibres are captured using the adhesive tape, see Figure 1(a) and Figure 1(b), ensuring that the single fibre projects perpendicularly to the edge of the adhesive tape. Second, the single fibre is positioned, see Figure 1(c), and aligned over the support chip, see Figure 1(d). A key point here is that the single fibre project perpendicularly from the polypropylene support chip. The alignment (<100 µm) was important as this is the crucial 'anchoring' of the cantilever [27,28]. Poorly aligned anchoring could result in spurious results. Therefore, a small pressure was then applied to

the adhesive tape to ensure good adhesion. The result is the final chip consisting of the single fibre based microcantilever aligned to the polypropylene chip, Figure 1(e). Figure 2 shows examples of the flax fibre-based cantilevers fabricated for the study.

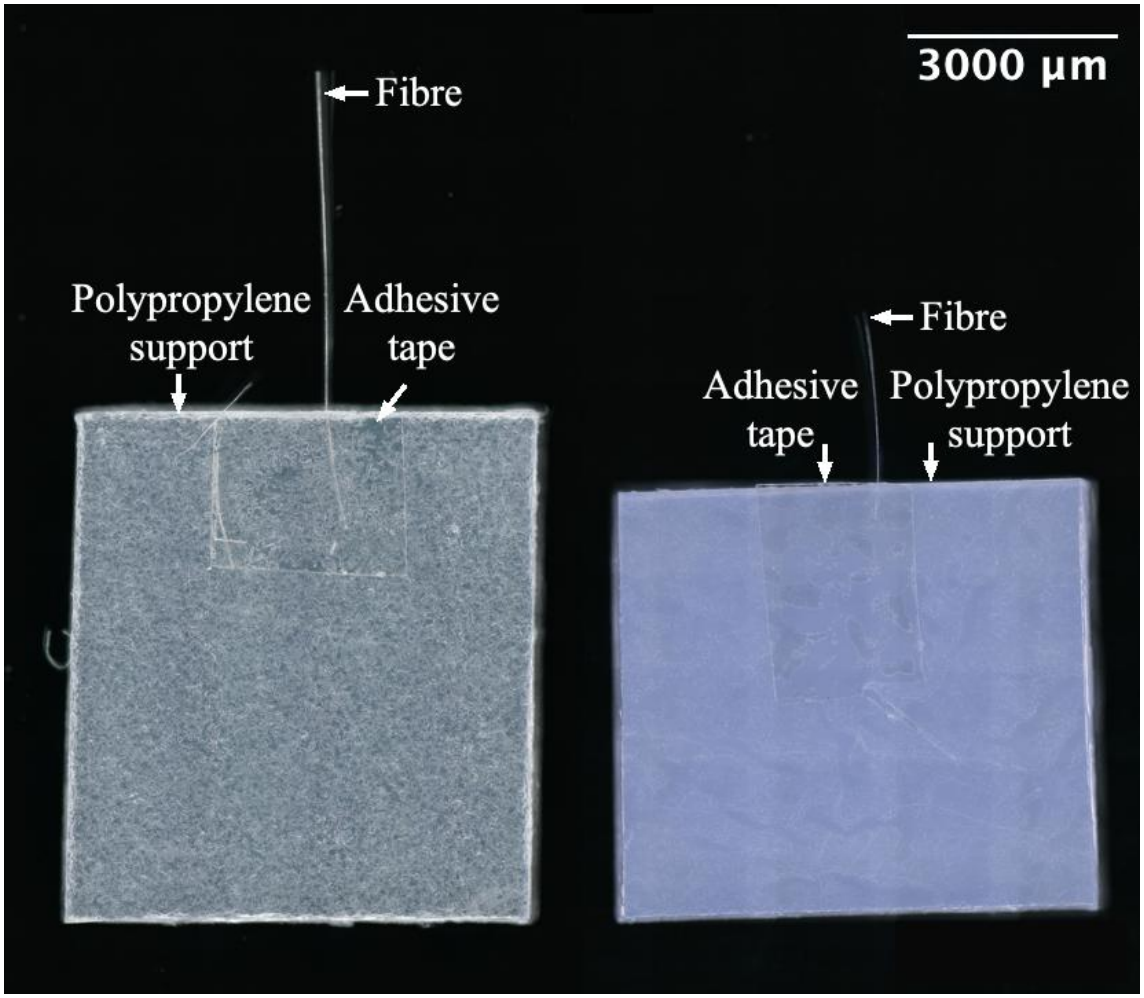

Figure 2. Digital optical microscope (DOM) images of examples of the cantilever/polypropylene support chip ensembles fabricated using our method. Single flax fibre-based cantilevers having a length of (left image) 4752 µm and (right image) 2426 µm. The diameter of the flax fibres tested in the study ranges from 20 µm to 55 µm.

To quantify the anchoring, we measured the adhesion pressure of our clamping tape to be 2.41×10^{5} N m^{-2}. For a clamping tape area of 2mm by 2mm, this corresponds to an adhesion force of ~1N, much greater than the bending forces of the deflecting cantilever, calculated to be a few tens of µN at maximum deflection. We can therefore consider the effect of anchoring adhesion to be negligible, and the anchoring to be quasi-rigid.

Prior to performing the experiments, the fibre diameter, along their entire length, was assessed using a VHX-6000 digital optical microscopy (Keyence, France) using a top view and a lateral side view of the fibre. The reason for doing this was to ensure the uniformity, homogeneity, and near-circular approximation of the single flax fibre cantilevers. Figure 3 shows digital optical microscopy images of an example of the fibre-based cantilever.

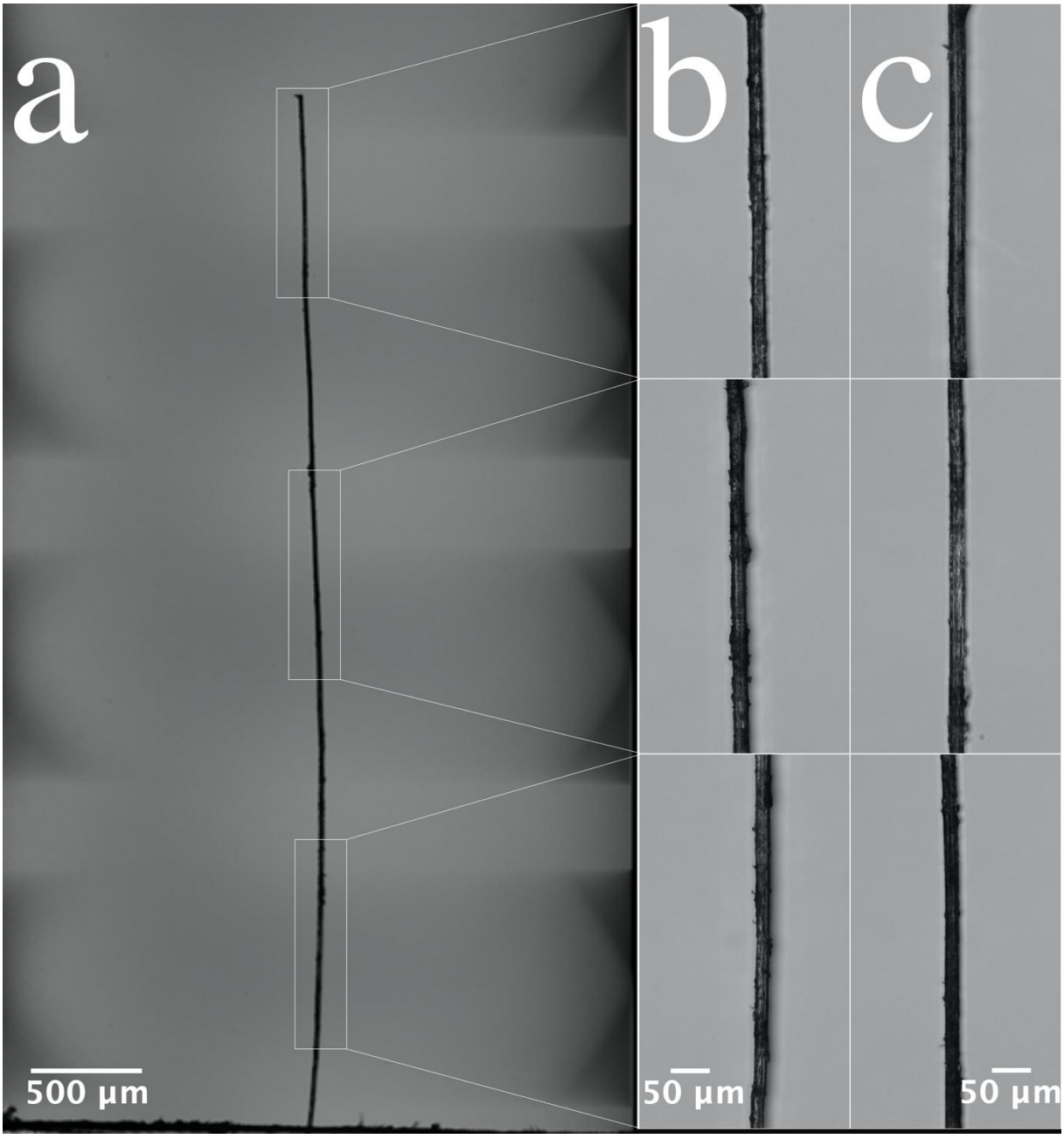

Figure 3. Digital optical microscopy images of an example of a fibre-based cantilever fabricated for the study. (a) Top view of the assembled cantilever showing the whole length. (b) Zoom images of the top view of three positions, and (c) zoom images of lateral side views of these positions.

Figure 3(a) shows a top view of the whole fibre which has a length of 4670 µm. Figure 3(b) and Figure 3(c) show zoomed images of top and lateral views of the single fibre; the average fibre diameter is 20.0±1.8 µm. For the mechanical model to be valid, the fibres must have a near-circular shape. Experimentally, this was achieved by assessing the fibre thickness of top and lateral views. When the top and the lateral average diameters had a difference of less than 5%, we considered the fibre to be near circular. The measurements suggest that the fibres are quasi-circular in cross sections.

Moreover, given the hollow nature of the flax fibre, it is essential to consider its effect on the mechanical behaviour. To quantify the hollowness and the near circularity of the fibres and know which model (pipe or solid cylinder) to apply, further experiments were undertaken to observe the fibre cross section. First, 1 cm length stem samples were embedded in London Resin (LR)-white acrylic resin (Sigma-France) and then the sections were cut with a diamond blade [29]. This method preserves the integrity of the fibre structure and allows easy microscopic examination of the fibre cross sections.

Figure 4 shows an example of cross-sections of the flax stem, providing a visual insight into the arrangement, distribution, and the cross-sectional shape of fibres within the structure.

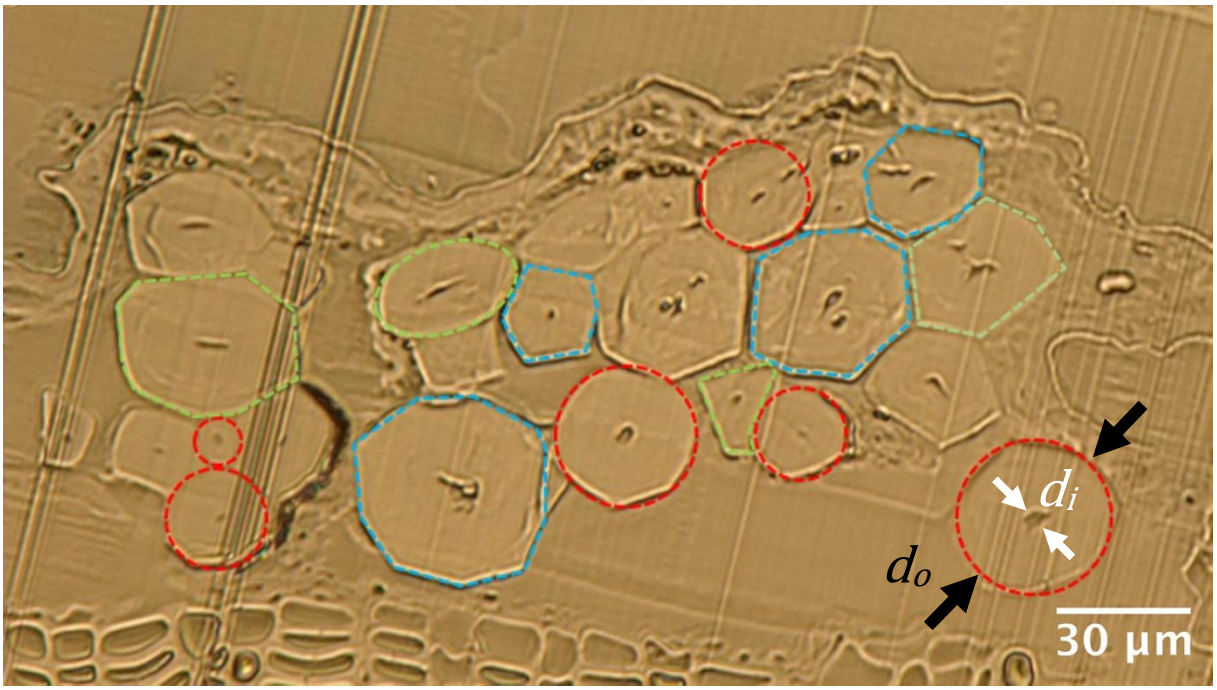

Figure 4. Digital optical microscopy image of cross sections of the flax fibres. The three principal cross-sectional shapes are circular (red), near circular (blue), and irregular (green). The outer and inner diameters of a flax fibre are shown by the black and white arrows.

Figure 4 clearly shows that many fibres have a near circular cross section. Indeed, our analysis of many cross-section samples enables the identification of three types of cross section: circular (red in Figure 4), polygonal which can be approximated by a circular cross section (blue in Figure 4), and irregular shapes that cannot be approximated by a circular cross section (green in Figure 4). This last category of fibres was excluded from the study by careful measurement of the top and lateral diameters of the mounted cantilever samples, as explained above.

In terms of the hollowness of the flax fibres, we observed that the average ratio of the inner diameter to the outer diameter is less than 0.12, based on 50 measurements of outer and inner diameters from digital microscopy images (see black and white arrows in Figure 4).

The next part of the paper presents the dynamic measurements of the fibre-based microcantilevers.

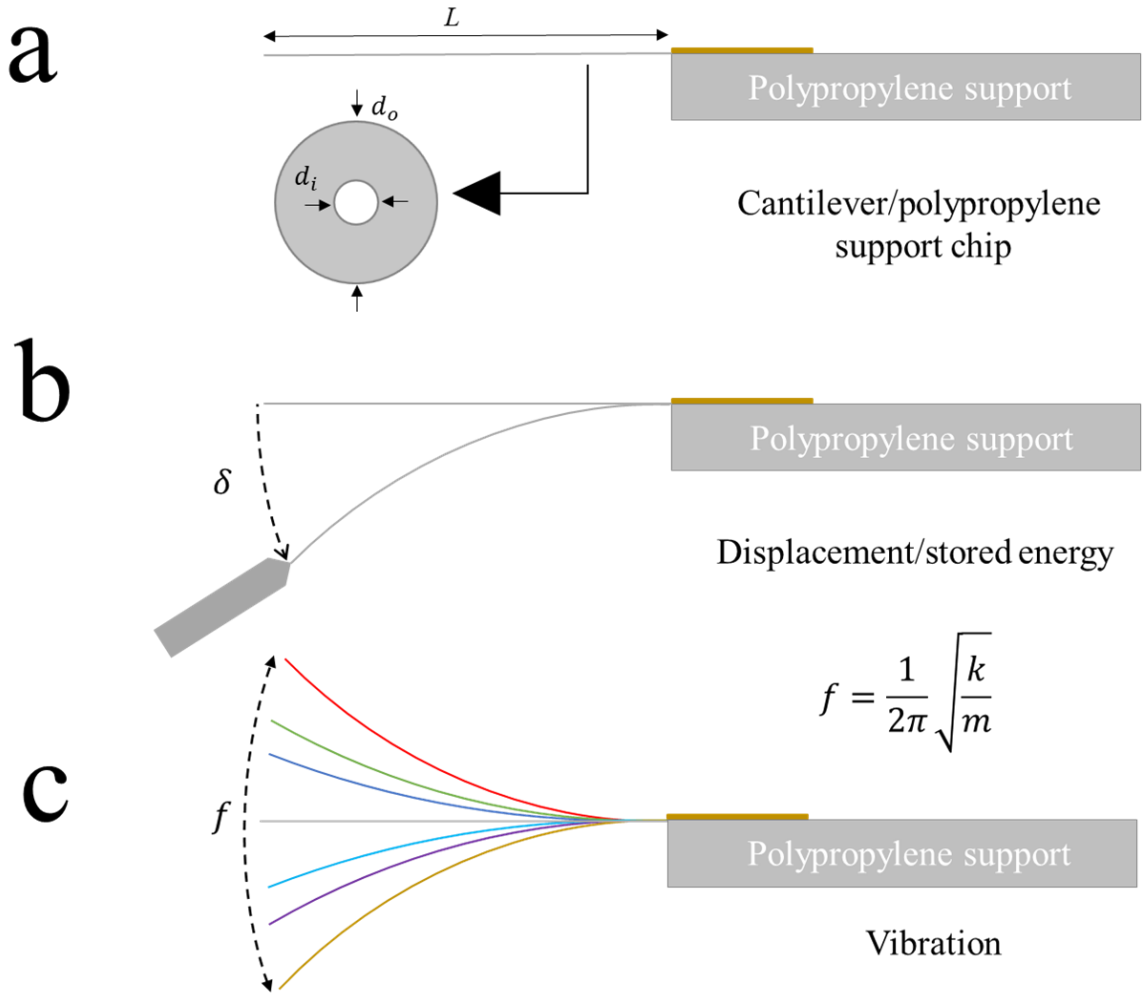

Figure 5. Schematic diagram showing the ideas. (a) A hollow cylinder-shaped fibre-based cantilever is mounted on a polypropylene support chip. (b) A displacement stimulator is used to give the cantilever stored potential energy. (c) Upon release the vibrational deflection of the fibre-based cantilever can be captured using high speed photography, analysis of this data gives the transient response of the cantilever.

Figure 5 illustrates the experimental setup used in this part of the study. A single fibre cantilever/support chip configuration is carefully mounted within a high-speed camera setup, in an air environment, see Figure 5(a). The high-speed camera was a 1280×800 pixels, frame rate = 3260 fps, ISO 7000 (Vision Research, USA). A displacement stimulator is then used to displace the cantilever a few hundred microns away from the central equilibrium position, causing potential stored energy to accumulate within the cantilever, see Figure 5(b). Upon release, the potential stored energy is dissipated, resulting in vibration cycles of the cantilever with diminishing amplitude due to

damping (primarily air), see Figure 5(c). Figure 6 shows high-speed camera images of a vibrating flax fibre-based cantilever.

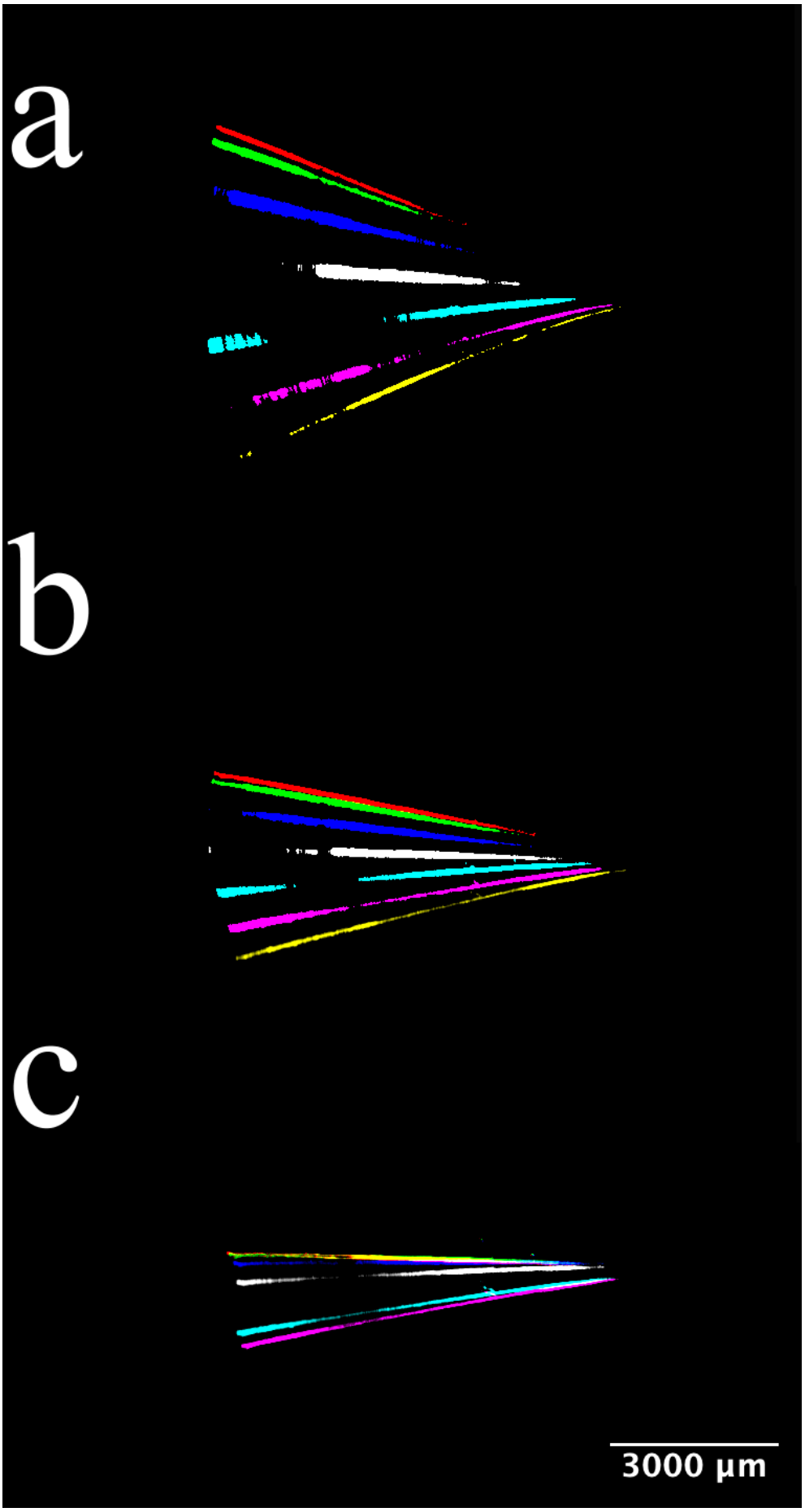
a
b
c
3000 µm

Figure 6. High-speed camera images of a vibrating flax fibre-based cantilever. (a) One half period in high amplitude regime, (b) and (c) one half periods in low amplitude regime. The cantilever has a length of 7547.1 µm and an average diameter of 20.93 µm. The time between each of the seven deflections shown (colours) is 312 µs.

Damping causes the transition from the high amplitude regime, Figure 6(a), to the low amplitude regime, Figure 6(c), passing through the limit between the two, Figure 6(b). The colours correspond to different deflections of the cantilever during one half cycle—delayed by 312 µs. The deflection is the only variable parameter during damping harmonic vibration of the cantilever. In the high amplitude regime, the amplitude measures 6009 µm, see Figure 6(a). Damping causes the system to move from the high amplitude regime to the low amplitude regime, resulting in a decrease in amplitude to 3373 mm, see Figure 6(b). Towards the end of the vibration, damping causes further reduction in amplitude to 1724 µm Figure 6(c), before returning to its initial state.

The transient response can be determined from the cantilever deflection data which was captured using the high-speed camera. Then, the transient response can be fitted with a function to determine the first mode natural frequency.

Using image analysis software [30], video tracking analysis plugins used to plot the transient response. It should be noted that in Figure 6 the fibre position is sometimes blurred at lower deflections, i.e. higher velocity); in this case the deflection is measured at the centre of the fibre images. The data obtained from the videos exhibit harmonic behaviour. Therefore, a damped harmonic model is used to fit the data. The damped harmonic system is modelled by:

$$A(t) = A_0 e^{-\beta t} cos\,(\omega t + \varphi) \tag{6}$$

This is plotted in red alongside the raw data over the same time span, represented by the open circles.

Figure 7 shows the total transient response of a flax fibre-based cantilever over 36 ms, from the release of the motion simulator to almost the point of fibre relaxation. The data points (open black circles) correspond to measurements of the cantilever deflection extracted from the high-speed camera data. The orange curve is obtained using a numerical fitting method of Equation 6. The best fitting curve minimises the sum of the squares of the differences between the measured and model values.

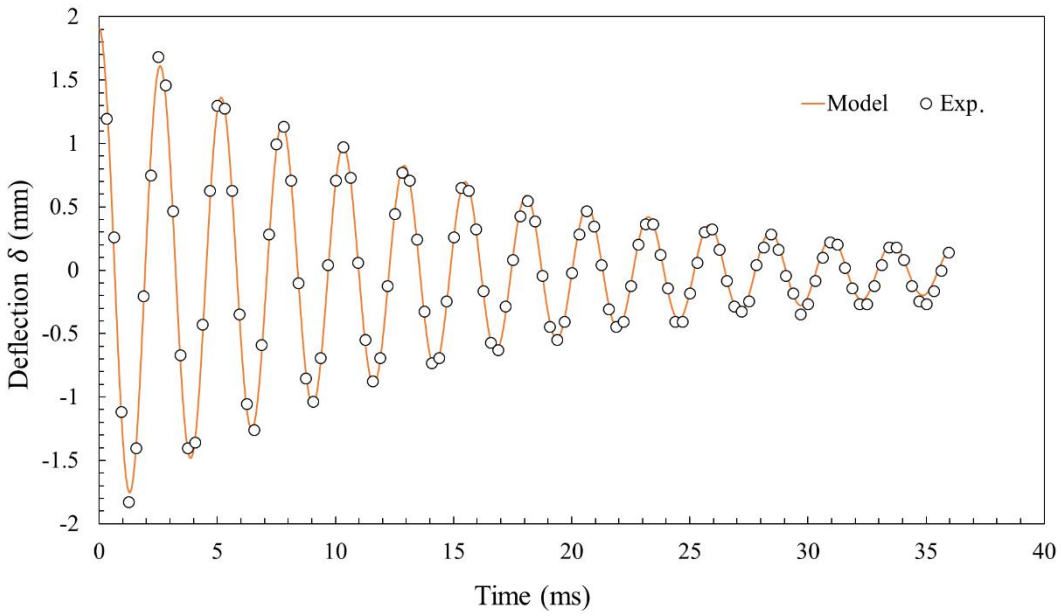

Figure 7. Transient response of the flax fibre-based cantilever. The open circles represent the raw data extracted from data analysis, and the orange curve represents a numerical fitting of the damped simple harmonic motion model in Equation 6.

However, before proceeding in determining the flexural modulus of the flax fibres, we must take three factors into account: (i) the influence of gravity on the initial bending, (ii) adherence to the low deflection regime (where the above solution is valid) and (iv) the contribution of air damping, something that can alter the frequency.

First, using an average density of the fibres (based on measured values found in the literature [31]), the mass of the largest fibre used is computed to be 2.9×10^{-8} Kg. The gravity force ($F = mg$) on the cantilever is 0.28 µN. If we consider a deflection of 0.5 mm, we compute a bending force of 22.5 µN. The contribution of gravity on the initial bending is therefore 1.2% of the total force and is negligible.

Second, the low deflection condition [25,26] must be met for the modelling to be valid. This means that the following inequality must be applied to the results:

$$\delta \leq 0.3L$$

Where δ is the deflection of the end of the cantilever and L is the length of the cantilever. By assessing the deflection where $\delta \leq 0.3L$, we can locate the low deflection regime in the damped harmonic system, as a function of time. For this particular flax fibre, the analysis revealed that the

maximum deflection, relative to $\delta \leq 0.3L$, was 1.6 mm. This marked the beginning of what we defined as the low deflection regime in our study.

Figure 8 shows the transient response of the flax fibre-based cantilever in the low deflection regime.

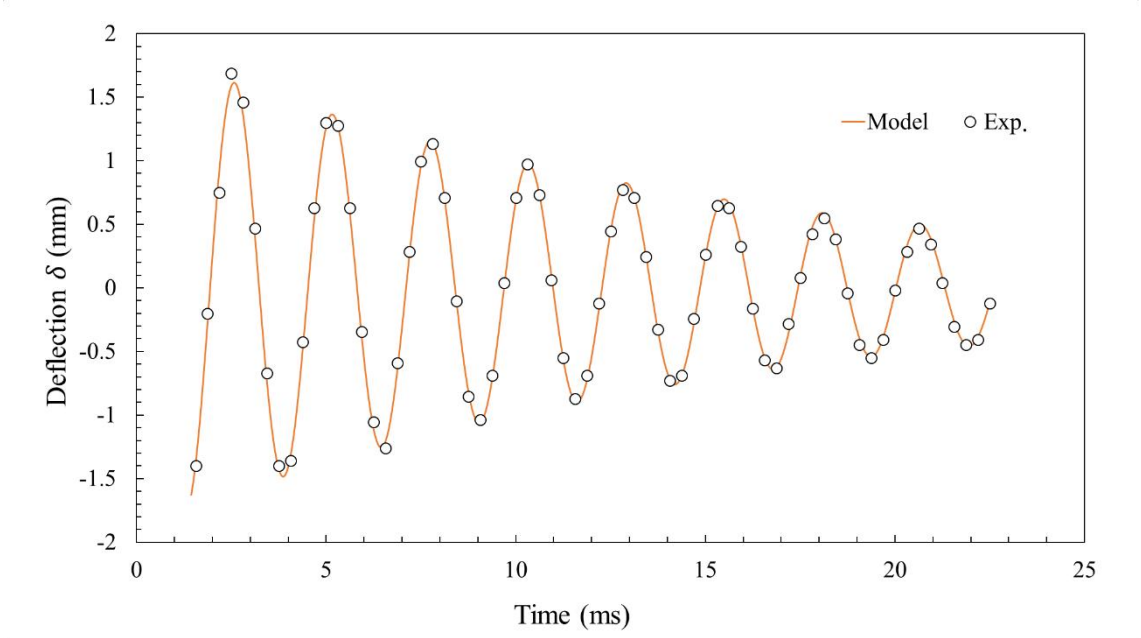

Figure 8. Transient response of the flax fibre-based cantilever in the low deflection regime. The open circles represent the raw data extracted from data analysis, and the orange curve represents a numerical fitting of the damped simple harmonic motion model in Equation 6.

This plot plays a crucial role in determining the harmonic frequency in the low deflection regime. Using the angular frequency value derived from numerically fitting the function in Equation 6 to the raw data, we can accurately determine the first mode harmonic frequency f associated with the damping that occurs in the low deflection regime by the familiar relationship:

$$f = \frac{\omega}{2\pi} \tag{7}$$

Third, air damping results in a shift of the resonant frequency—this is true for macroscopic [32] and microscopic [33] cantilevers. This shift, if non-negligible, would lead to an error in the estimation of the bending modulus. Let us now estimate the shift in frequency due to air damping in our vibrating fibres.

The Reynolds number Re of the system is given by [34]:

$$Re = \frac{2\pi f \rho_{air} d_o^2}{\mu_{air}} \quad (8)$$

Where ρ and μ are the density and the dynamic viscosity of air. Using commonly known values (ρ_{air} = 1.293 kg m^{-3} and μ_{air} = 1.85×10^{-5} Pa s), an average frequency of the measurements of 268.4 Hz, and an average fibre diameter of 30.9 µm (of all samples tested), we have Re = 0.11.

This means that the following equation can be used to estimate the shift in the frequency, and therefore the error in computing the flexural modulus, due to air damping [35]:

$$\frac{f_{air}}{f_0} = \sqrt{1 - \frac{1}{4Q^2}} \quad (9)$$

Where f_{air} is the resonant frequency in the presence of air damping and f_0 is the resonant frequency in the absence of air damping, and Q is the quality factor of the damped harmonic system

$$Q = \frac{\omega}{2\alpha} \quad (10)$$

The experimentally-determined average quality factor Q was 8.7, i.e. the ratio f_{air}/f_0 = 0.998. Therefore, air damping does not lead to a large error (<1%) in the determination of the flexural modulus of the fibres using this method. This means that the following equation is valid to compute the value of the flexural modulus from the experimental measurements:

$$E_f = \left(\frac{2\pi f_{air}}{\alpha_1^2}\right)^2 \frac{16\rho L^4}{d_o^2 + d_i^2} \quad (11)$$

Based on measurements of 18 fibre samples, the flexural modulus of the individual flax fibres was determined. Table 1 shows the sample number and corresponding measurements of each sample.

Table 1. Summary of experiments.

Sample	d_o (µm)	d_i (µm)	f_{air} (Hz)	L (µm)	E_f (GPa)
1	46.56	5.59	385.56	7625.0	15.82
2	55.45	6.65	362.23	8862.5	17.97
3	20.08	2.41	180.60	8517.1	29.05
4	36.91	4.43	190.03	10145.7	19.17
5	26.14	3.14	214.97	7900.1	17.98
6	24.55	2.94	302.55	6828.2	22.53
7	30.25	3.63	326.43	7748.8	28.65

8	40.05	4.80	348.73	7509.2	16.45
9	27.54	3.30	338.19	6988.9	24.56
10	22.16	2.66	210.14	8167.3	27.31
11	24.59	2.95	148.98	9943.6	24.49
12	20.93	2.51	243.07	7547.1	29.86
13	33.92	4.07	160.83	9980.7	15.23
14	25.03	3.00	313.69	7629.2	36.32
15	28.40	3.41	111.47	10852.3	14.58
16	35.95	4.31	501.98	6849.6	29.29
17	25.07	3.01	276.07	7921.3	32.58
18	33.20	3.98	214.83	8706.4	16.42

As a result, the model was able to accurately determine a flexural modulus of the flax fibres to be 23.24 GPa for a fibre outer diameter range of approximately 20-55 µm, see Table 2.

Table 2. Summary of results. d_o^{range} is the outer diameter range, E_f^{ave} is the average flexural modulus, and S.D. is the standard deviation of the results.

d_o^{range} (µm)	E_f^{ave} (GPa)	*S.D.*
20.08-55.45	23.24	6.78

4. Discussions

In terms of fibre homogeneity, flax fibres are not homogenous but rather heterogeneous structures [13] composed of different layers, i.e. the primary cell wall and the secondary cell wall, see Figure 9. The approach here cannot measure the individual mechanical properties of these component parts. The heterogeneity is reflected in its chemical composition but physically, and for mechanical modelling purposes, it is considered to be homogenous [36,37]. When considering the fibre as a pipe, we made every effort to characterise its physical homogeneity, i.e. its outside diameter and the importance of the lumen size inside the fibre. In as much, the techniques here accurately measure the composite modulus of the heterogeneous fibre.

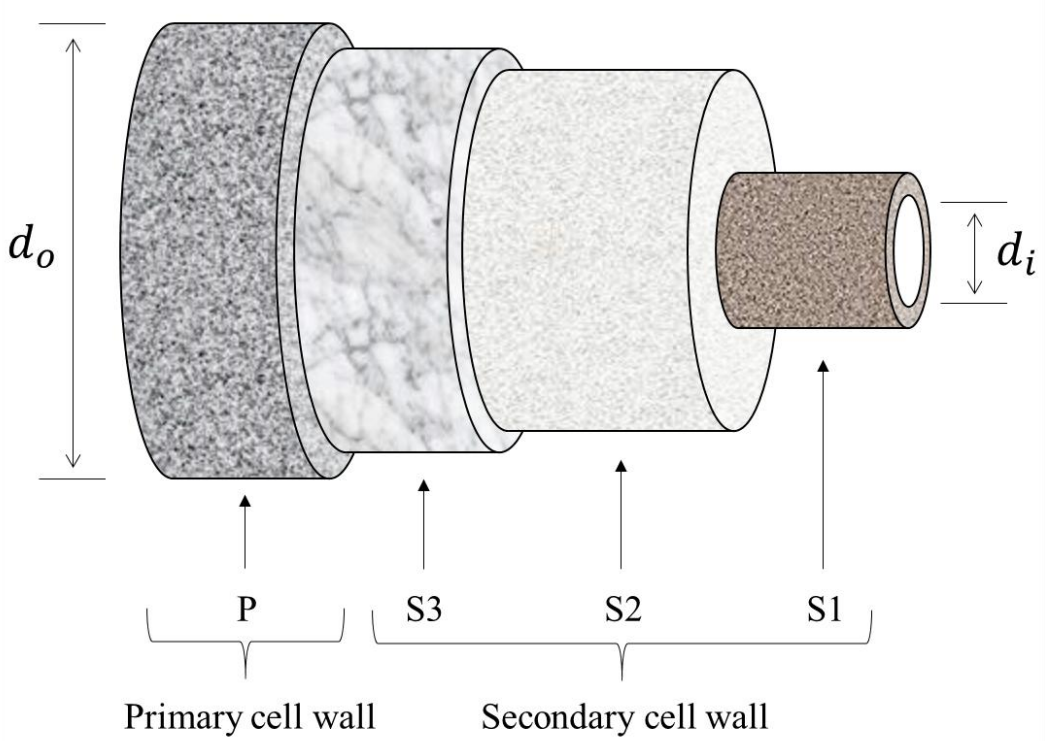

Figure 9. Internal structure of a flax fibre.

In terms of the modulus, many authors have reported values between 20-80 GPa using tensile techniques, e.g. Charlet *et al.* [15]. However, our results agree well with previously reported values of the elastic modulus of flax fibres [36,37] at the lower end of this range of the reported values; knowing that the value comes from work originally published in 1982 [38].

In terms of data scatter, the error in the results is better than that which would be obtained using macro-mechanical testing, e.g. tensile testing, where one would typically expect 50-100 %. Charet *et al.* [15] presented interesting results for the evolution of the Young's (tensile) modulus of flax fibres as a function of fibre diameter using tensile testing–this data in Figure 10 in solid squares. By analysing their results, the range of moduli is 21.6-89.2 GPa, with a downward trend of -1.19 GPa μm^{-1}. This actually agrees quite well with our findings as the majority of our fibres have an outer diameter greater than 25 µm (13 out of 18). By plotting our results in a similar way, we find that our flexural modulus range is 13.98-34.83 GPa with a downward trend of -0.38 GPa μm^{-1}, see Figure 10.

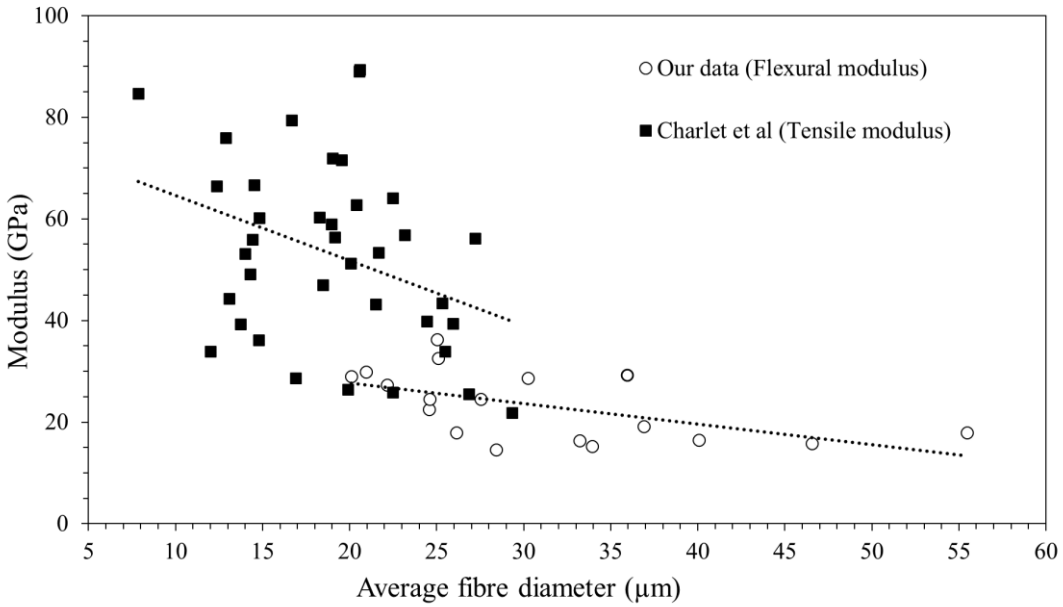

Figure 10. Plot of the flexural modulus as a function of average fibre diameter (our data, open circles). As a comparison, the tensile modulus reported by Charlet et al [15] is also plotted (solid squares).

The success of our microscale approach extends beyond the precise determination of modulus. It is well known that natural fibres, such as flax, often acquire numerous defects (especially when preparing long samples for tensile testing) that can significantly affect their mechanical properties, leading to data scatter. In our approach, we strategically reduced the sample length tested from a few centimetres, as typically used in tensile testing, to a few millimetres. This aspect played a key role in improving the accuracy and reliability of the modulus extraction using modelling. Thus, using our micro-scale method, we achieved good precision with error bars and standard deviations in the relatively narrow range of ±6 GPa, a significant improvement over the wider range often observed in standard traditional tensile tests on longer samples, where large scatter and dispersion in data is seen. The results obtained from our approach thus demonstrate the effectiveness of our strategy inspired by MEMS testing in achieving accurate characterisation of flax fibre properties while minimising the potential disturbances arising from inherent structural irregularities.

In terms of model, this study demonstrates that the proposed modelling, initially validated for the low deflection regime, can be reliably extended to accurately extract the modulus even in the high deflection regime. We observed that the performance of the model in the high deflection regime, where the deflections are still relatively small compared to the total fibre length, gave

accurate and consistent results. Our results show no frequency shift between the high and low deflection regimes, indicating that it remains robust and applicable for deflections up to 30% of the fibre length. Our results successfully validated our assumption and the use of the damped harmonic vibration model, which proved to be highly effective in extracting the flexural modulus of the flax fibre. Importantly, this micro-scale approach allowed us to accurately determine the fibre flexural modulus even for small fibre lengths, resulting in significantly reduced data scatter compared to conventional macro-scale mechanical tests such as tensile testing.

Finally, in terms of dynamic measurements. To our knowledge, there are no dynamic studies on microscopic single flax fibres using a cantilever and a high-speed camera. Gnec *et al.* [39] used dynamic techniques to measure the mechanical modulus of flax fibre composites. They quote a value of 30 GPa (near to that reported here) for the fibre modulus and around 10 GPa for the fibre/resin composite. Interestingly their errors are relatively small (as reported here using dynamic techniques) compared to tensile testing. However, the materials used in the study are a commercial composite flax fabric of Hermes variety–not the same species as ours.

5. Conclusion

In conclusion, our dynamic micromechanical MEMS-inspired approach proves to be a robust and accurate method for extracting the flexural modulus of fibres, including natural fibres and even hair, based on deflection analysis. This study shows that the fabrication and mounting of the samples using polypropylene chips and Scotch tape is straightforward, inexpensive and fast. However, we found that the extraction of single flax fibre samples required careful attention to avoid the presence of multiple fibres, which could affect the accuracy of the measurements. The fabrication process itself is simple, involving the use of a polypropylene chip and the attachment of the flax fibre sample perpendicular to the edge of the chip. Microscope assistance during fabrication ensured that the fibre was accurately attached to the edge of the chip, i.e. anchoring length << L, thus avoiding any spurious effects due to poor cantilever anchoring. In terms of measurements, this technique offers an easy setup compared to macroscopic testing, e.g. tensile tests, requiring only a high-speed camera to record the transient response of the cantilever. Subsequent analysis of the data is straightforward, facilitated by image analysis software that allows us to track the maximum deflection of the tip of the cantilever. Digital optical microscopy enables a control of fibre uniformity, homogeneity, and dimensions. In this study, flax fibres were approximated to a hollow pipe structure, which allowed us to use analytical modelling to accurately determine the flexural modulus from the natural vibration frequency. However, it is important to acknowledge that this method does not allow the direct

extraction of fibre breaking stress due to the limitation of deflection as the sole parameter. In order to gain a more comprehensive understanding of fibre strength, it is imperative to research and develop alternative powerful methods that can facilitate the extraction of fibre breaking stress. Such methods would provide valuable insights into the mechanical integrity and performance of fibres, further enhancing our knowledge for the diverse applications of natural fibres in modern thermoplastic and industrial materials. One potential avenue for extracting fibre flexural stress is to adapt static micromechanics methods. By taking into account various fibre characteristics, including dimensions, structure, manipulation, homogeneity and density, these adapted methods could offer a promising approach to uncover the breaking stress and provide a more comprehensive picture of fibre strength. Overall, our study highlights the effectiveness of the dynamic micromechanical approach to accurate flexural modulus determination and emphasises the importance of exploring novel techniques to access additional mechanical parameters, ultimately advancing our understanding and use of natural fibres in diverse applications. Through continued research and innovation, we can expand our understanding of fibre mechanics and contribute to the development of more efficient and robust materials in various industrial and engineering fields.

Acknowledgement

Many thanks to the company Van Robaeys Frères (Killem, France) for allowing us to collect flax stem samples from their fields. We also thank Lionel Buchaillot and Anne-Marie Blanchenet (UMET-CNRS, University of Lille) for cutting certain stem samples used for cross-section imaging. The authors thank Sebastien Grec and Simon Hawkins (UGSF-CNRS, University of Lille) for their help in stimulating and facilitating the collaboration between IEMN and Van Robaeys Frères, and also for supplying the flax stem storage equipment during travelling to a from the field. We thank Vincent Thomy (Prof. at Univ. Lille) for the loan of the high-speed camera.

References

[1] Qian G-L, Hoa S V and Xiao X 1997 A vibration method for measuring mechanical properties of composite, theory and experiment *Composite Structures* **39** 31–8

[2] Mantena P R 1996 Frequency Domain Vibration Analysis For Characterizing The Dynamic Mechanical Properties Of Materials *1996 Annual Conference Proceedings* 1996 Annual Conference (Washington, District of Columbia: ASEE Conferences) p 1.222.1-1.222.7

[3] Bediz B, Nevzat Özgüven H and Korkusuz F 2010 Vibration measurements predict the mechanical properties of human tibia *Clinical Biomechanics* **25** 365–71

[4] Prabhakaran S, Krishnaraj V, Kumar M S and Zitoune R 2014 Sound and Vibration Damping Properties of Flax Fiber Reinforced Composites *Procedia Engineering* **97** 573–81

[5] Ward I M and Sweeney J 2013 *Mechanical properties of solid polymers* (Chichester, West Sussex, United Kingdom: Wiley)

[6] Sundararajan S and Bhushan B 2002 Development of AFM-based techniques to measure mechanical properties of nanoscale structures *Sensors and Actuators A: Physical* **101** 338–51

[7] Espinosa H D, Prorok B C, Peng B, Kim K H, Moldovan N, Auciello O, Carlisle J A, Gruen D M and Mancini D C 2003 Mechanical properties of ultrananocrystalline diamond thin films relevant to MEMS/NEMS devices *Experimental Mechanics* **43** 256–68

[8] Bertke M, Fahrbach M, Hamdana G, Xu J, Wasisto H S and Peiner E 2018 Contact resonance spectroscopy for on-the-machine manufactory monitoring *Sensors and Actuators A: Physical* **279** 501–8

[9] Jaquez-Moreno T, Aureli M and Tung R C 2019 Contact Resonance Atomic Force Microscopy Using Long, Massive Tips *Sensors* **19** 4990

[10] Sheehy M, Punch J, Goyal S, Reid M, Lishchynska M and Kelly G 2009 The Failure Mechanisms of Micro-Scale Cantilevers Under Shock and Vibration Stimuli *Strain* **45** 283–94

[11] Fu J, Lin L, Zhou X, Li Y and Li F 2012 A macroscopic non-destructive testing system based on the cantilever-sample contact resonance *Review of Scientific Instruments* **83** 123707

[12] Rabe U, Janser K and Arnold W 1996 Vibrations of free and surface-coupled atomic force microscope cantilevers: Theory and experiment *Review of Scientific Instruments* **67** 3281–93

[13] Baley C 2002 Analysis of the flax fibres tensile behaviour and analysis of the tensile stiffness increase *Composites Part A: Applied Science and Manufacturing* **33** 939–48

[14] Charlet K, Baley C, Morvan C, Jernot J P, Gomina M and Bréard J 2007 Characteristics of Hermès flax fibres as a function of their location in the stem and properties of the derived unidirectional composites *Composites Part A: Applied Science and Manufacturing* **38** 1912–21

[15] Charlet K, Eve S, Jernot J P, Gomina M and Breard J 2009 Tensile deformation of a flax fiber *Procedia Engineering* **1** 233–6

[16] Yan L, Chouw N and Jayaraman K 2014 Flax fibre and its composites – A review *Composites Part B: Engineering* **56** 296–317

[17] Richely E, Bourmaud A, Placet V, Guessasma S and Beaugrand J 2022 A critical review of the ultrastructure, mechanics and modelling of flax fibres and their defects *Progress in Materials Science* **124** 100851

[18] Yoo W-S, Lee J-H, Park S-J, Sohn J-H, Dmitrochenko O and Pogorelov D 2003 Large Oscillations of a Thin Cantilever Beam: Physical Experiments and Simulation Using the Absolute Nodal Coordinate Formulation *Nonlinear Dynamics* **34** 3–29

[19] Basu A K, Sah A N, Pradhan A and Bhattacharya S 2019 BSA Detection on Polymeric Nanocantilever *Advances in Interdisciplinary Engineering* Lecture Notes in Mechanical Engineering ed M Kumar, R K Pandey and V Kumar (Singapore: Springer Singapore) pp 589–94

[20] Pang T Y, Subic A and Takla M 2011 Finite element analysis of impact between cricket ball and cantilever beam *Procedia Engineering* **13** 258–64

[21] Zhang C, Zhou H, Xu L, Ru Y, Ju H and Chen Q 2022 Measurement of morphological changes of pear leaves in airflow based on high-speed photography *Front. Plant Sci.* **13** 900427

[22] Shah D U, Reynolds T P and Ramage M H 2017 The strength of plants: theory and experimental methods to measure the mechanical properties of stems ed C Raines *Journal of Experimental Botany* **68** 4497–516

[23] Schramm M, Tekeste M Z, Plouffe C and Harby D 2019 Estimating bond damping and bond Young's modulus for a flexible wheat straw discrete element method model *Biosystems Engineering* **186** 349–55

[24] Shioya M, Myoga A, Kitagawa A, Tokunaga Y, Hayashi H, Kogo Y, Shimada H and Satake S 2019 Analysis of deflection and dynamic plant characteristics of *Cyperus malaccensis* Lam *Plant Production Science* **22** 242–9

[25] Timoshenko S 2010 *Theory of elasticity* (New Delhi, India: McGraw-Hill Education)

[26] Young W C and Budynas R G 2002 *Roark's formulas for stress and strain* (New York: McGraw-Hill)

[27] Davis Z J, Svendsen W and Boisen A 2007 Design, fabrication and testing of a novel MEMS resonator for mass sensing applications *Microelectronic Engineering* **84** 1601–5

[28] Lee J E-Y, Yan J and Seshia A A 2011 Study of lateral mode SOI-MEMS resonators for reduced anchor loss *J. Micromech. Microeng.* **21** 045010

[29] Goudenhooft C, Siniscalco D, Arnould O, Bourmaud A, Sire O, Gorshkova T and Baley C 2018 Investigation of the Mechanical Properties of Flax Cell Walls during Plant Development: The Relation between Performance and Cell Wall Structure *Fibers* **6** 6

[30] Schindelin J, Arganda-Carreras I, Frise E, Kaynig V, Longair M, Pietzsch T, Preibisch S, Rueden C, Saalfeld S, Schmid B, Tinevez J-Y, White D J, Hartenstein V, Eliceiri K, Tomancak P and Cardona A 2012 Fiji: an open-source platform for biological-image analysis *Nat Methods* **9** 676–82

[31] Bourmaud A, Mérotte J, Siniscalco D, Le Gall M, Gager V, Le Duigou A, Pierre F, Behlouli K, Arnould O, Beaugrand J and Baley C 2019 Main criteria of sustainable natural fibre for efficient unidirectional biocomposites *Composites Part A: Applied Science and Manufacturing* **124** 105504

[32] Baker W E, Woolam W E and Young D 1967 Air and internal damping of thin cantilever beams *International Journal of Mechanical Sciences* **9** 743–66

[33] Albrecht T R, Akamine S, Carver T E and Quate C F 1990 Microfabrication of cantilever styli for the atomic force microscope *Journal of Vacuum Science & Technology A: Vacuum, Surfaces, and Films* **8** 3386–96

[34] Batchelor G K 2010 *An Introduction to fluid dynamics* (Cambridge: Cambridge Univ. Press)

[35] Sader J E, Larson I, Mulvaney P and White L R 1995 Method for the calibration of atomic force microscope cantilevers *Review of Scientific Instruments* **66** 3789–98

[36] Mohanty A K, Misra M and Hinrichsen G 2000 Biofibres, biodegradable polymers and biocomposites: An overview *Macromol. Mater. Eng.* **276–277** 1–24

[37] Faruk O, Bledzki A K, Fink H-P and Sain M 2012 Biocomposites reinforced with natural fibers: 2000–2010 *Progress in Polymer Science* **37** 1552–96

[38] Sridhar M K, Basavarajappa G, Kasturi S G and Balasubramanian N 1982 Evaluation of jute as a reinforcement in composites *Indian J. Text. Res.* **7** 87–92

[39] Gnec G, El Hafidi A and Gning P 2012 Comparison of the mechanical properties of flax and glass fiber composite materials *J. Vibroengineering* **14** 572–81